Cryptand Cage: Perfect Skeleton for Transition Metal Induced Two-step Fluorescence Resonance Energy Transfer

Kalyan K. Sadhu[†], Subhasree Banerjee[‡], Anindya Datta[‡] and Parimal K. Bharadwaj[*,†]

[†]*Chemistry Department, Indian Institute of Technology Kanpur, Kanpur 208016 India*
[‡] *Chemistry Department, Indian Institute of Technology Bombay, Powai, Mumbai 400076 India*
Email: pkb@iitk.ac.in

Supporting Information

Experimental Section

Materials

All solvents and thionyl chloride were purified prior to use. The purified solvents were found to be free from impurities, moisture and were transparent in the region of interest. All other reagent grade chemicals including metal salts were acquired from Aldrich that were used as received. The metal salts were hydrated as mentioned in the Aldrich catalogue. For chromatographic separation, 100-200 mesh silica gel (Acme Synthetic Chemicals) was used. The reactions were carried out under N_2 atmosphere unless otherwise mentioned.

Synthesis. The synthetic route for the cryptand derivatives is illustrated in Scheme S1.

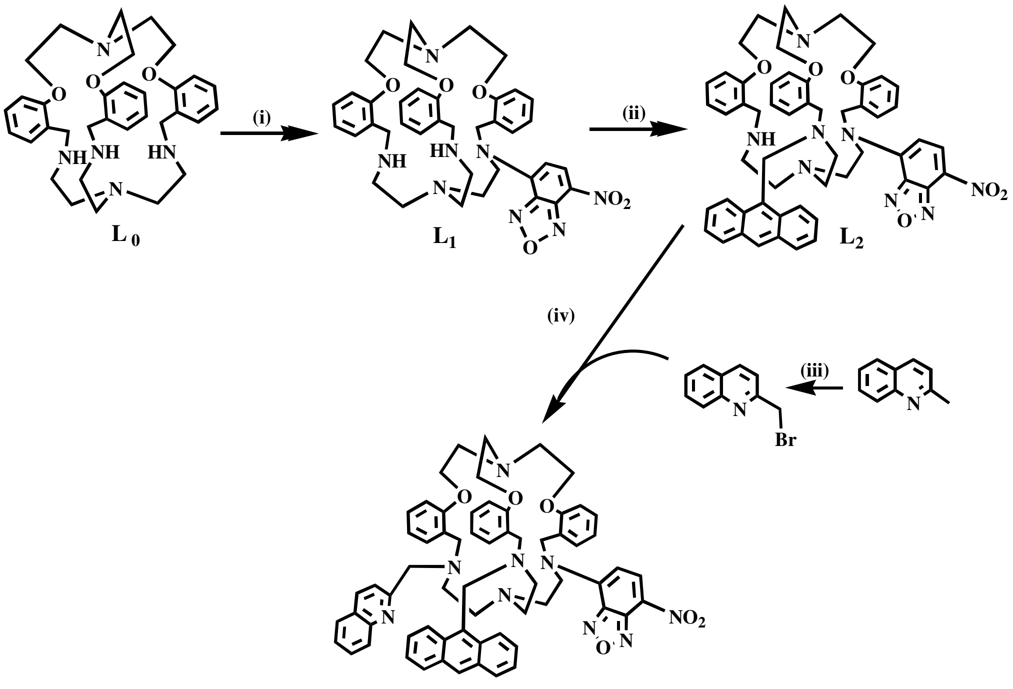

Scheme S1

Reagent and conditions: *(i)* 4-chloro 7-nitrobenz-2-oxa-1,3-diazole, Toluene, reflux 6 h. *(ii)* 9-Bromomethylanthracene, K_2CO_3, MeCN, KI, reflux, 48 h. (iii) NBS, CCl4, AIBN, 9 h. light.

Cryptand $\mathbf{L_0}$ was synthesized and recrystallized from acetonitrile as colorless rectangular crystals following our previously reported[S1] procedure.

Synthesis of L_1 and L_2. Compound $\mathbf{L_1}$ and $\mathbf{L_2}$ were synthesized following the procedure reported previously[S2] from our laboratory.

Synthesis of L: To a solution of $\mathbf{L_2}$ (0.46 g; 0.5 mmol) in dry acetonitrile (20 ml), anhydrous K_2CO_3 (1.5 g, excess) was added and stirred for 15 min. Freshly recrystallized 2-bromomethyl quinoline[S3] (0.11 g, 0.5 mmol) was added to it along with a crystal of KI and the reaction mixture was allowed to reflux for 72 h. After cooling to RT, K_2CO_3 was removed by filtration. The red filtrate was evaporated to dryness under reduced pressure, washed several times with water and then extracted with $CHCl_3$. The organic layer, after drying over anhydrous Na_2SO_4, evaporated to dryness to obtain a dark red solid as **L**.

Yield: 65(%); mp: 150 °C; ^{1}H-NMR (400 MHz, $CDCl_3$, 25 °C, TMS, δ): 1.23 (m, 8H, 4 × CH_2), 1.59 (m, 8H, 4 × CH_2), 2.04 (m, 8H, 4 × CH_2), 4.10 (s, 2H, CH_2), 4.75 (s, 2H, CH_2), 5.39 (s, 2H, CH_2), 5.80 (s, 2H, An-CH_2), 5.93 (s, 2H, Q-CH_2), 6.91 (m, 3H, 3 × Ar-H), 7.02 (d, 1H, 1 × D-H), 7.45 (m, 2H, 2 × An-H), 7.54 (m, 3H, 3 × Ar-H), 7.72 (m, 4H, 1 × Q-H, 3 × Ar-H), 7.82 (m, 4H, 2 × Q-H, 2 × An-H), 7.91 (m, 4H, 2 × Q-H, 2 × An-H), 8.07 (m, 4H, 1 × Q-H, 3 × Ar-H), 8.21 (m, 2H, 2 × An-H), 8.28 (m, 2H, 1 × D-H, 1 × An-H); ^{13}C-NMR (100 MHz, $CDCl_3$, 25 °C, TMS, δ): 168.63, 166.01, 159.96, 157.33, 156.98, 143.49, 134.23, 132.88, 132.13, 131.73, 131.27, 131.20, 131.13, 130.52, 129.42, 129.26, 128.97, 128.82, 128.56, 127.31, 127.02, 126.24, 125.81, 125.49, 125.21, 122.18, 121.18, 120.77, 111.61, 110.70, 76.91, 66.59, 65.30, 56.89, 55.12, 54.61, 53.56, 52.44, 47.74, 46.55, 45.52, 29.77, 28.73; ESI-MS (m/z): 1054 (100 %) $[\mathbf{L}]^+$. Anal. Calcd. for $C_{64}H_{63}N_9O_6$: C, 72.91; H, 6.02; N, 11.96 %. Found: C, 73.00; H, 6.04; N, 11.84 %.

Synthesis of 1, 2 and 3.

The synthetic route for the cryptand derivatives is illustrated in Scheme S2.

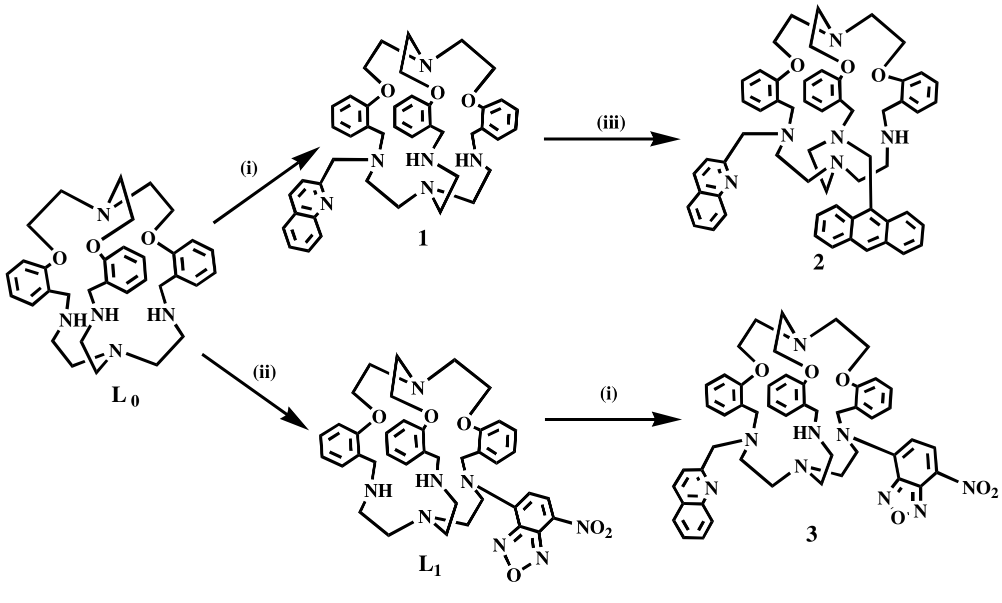

Scheme S2

Reagent and conditions: (i) 2-Bromomethylquinoline, K_2CO_3, MeCN, KI, reflux, 72 h. *(ii)* 4-chloro 7-nitrobenz-2-oxa-1,3-diazole, Toluene, reflux 6 h. *(iii)* 9-Bromomethylanthracene, K_2CO_3, MeCN, KI, reflux, 48 h.

Synthesis of 1: To a solution of **L_0** (0.28 g; 0.5 mmol) in dry acetonitrile (20 ml), anhydrous K_2CO_3 (1.5 g, excess) was added and stirred for 15 min. Freshly recrystallized 2-bromomethyl quinoline[S3] (0.11 g, 0.5 mmol) was added to it along with a crystal of KI and the reaction mixture was allowed to reflux for 72 h. After cooling to RT, K_2CO_3 was removed by filtration. The yellowish filtrate was evaporated to dryness under reduced pressure, washed several times with water and then extracted with $CHCl_3$. The organic layer, after drying over anhydrous Na_2SO_4, evaporated to dryness to obtain a faint yellow solid. Compound **1** was isolated as white solid through column chromatography.

Yield: 40(%); mp: 88 °C; ^{1}H-NMR (400 MHz, $CDCl_3$, 25 °C, TMS, δ): 0.85 (m, 4H, 2 × CH_2), 1.24 (m, 8H, 4 × CH_2), 1.58 (m, 4H, 2 × CH_2), 2.02-2.32 (m, 2H, CH_2), 4.07-4.21 (m, 2H, CH_2), 4.47 (br, 2H, 2 × NH), 4.92 (s, 6H, 3 × CH_2), 5.33 (s, 2H, Q-CH_2), 7.13 (m, 4H, 1 × Q-H, 3 × Ar-H), 7.24 (m, 2H, 2 × Q-H), 7.34 (m, 4H, 1 × Q-H, 3 × Ar-H), 7.51 (m, 4H, 1 × Q-H, 3 × Ar-H), 7.71 (m, 4H, 1 × Q-H, 3 × Ar-H); ^{13}C-NMR (100 MHz, $CDCl_3$, 25 °C, TMS, δ): 155.47, 144.42, 134.61, 123.09, 121.47, 112.09, 64.58, 32.02, 29.79, 29.45, 22.79, 14.22; ESI-MS (m/z): 701 (50 %) [**1**]$^+$. Anal. Calcd. for $C_{43}H_{52}N_6O_3$: C, 73.68; H, 7.48; N, 11.99 %. Found: C, 73.70; H, 7.44; N, 11.94 %.

Synthesis of 2: To a solution of **1** (0.35 g; 0.5 mmol) in dry acetonitrile (20 ml), anhydrous K_2CO_3 (1.5 g, excess) was added and stirred for 15 min. Freshly recrystallized 9-bromomethyl anthracene[S4] (0.14 g, 0.5 mmol) was added to it along with a crystal of KI and the reaction mixture was allowed to reflux for 72 h. After cooling to RT, K_2CO_3 was removed by filtration. The yellow filtrate was evaporated to dryness under reduced pressure, washed several times with water and then extracted with $CHCl_3$. The organic layer, after drying over anhydrous Na_2SO_4, evaporated to dryness to obtain a yellow solid. Compound **2** was isolated as yellow solid through column chromatography.

Yield: 35(%); mp: 126 °C; ^{1}H-NMR (400 MHz, $CDCl_3$, 25 °C, TMS, δ): 2.50 (m, 8H, 4 × CH_2), 2.71 (m, 8H, 4 × CH_2), 2.99 (m, 8H, 4 × CH_2), 3.89 (s, 6H, 3 × CH_2), 4.17 (br, 1H, NH), 4.69 (s, 2H, An-CH_2), 5.27 (s, 2H, Q-CH_2), 6.84 (m, 5H, 2 × An-H, 3 × Ar-H), 6.94 (m, 5H, 2 × An-H, 3 × Ar-H), 7.15 (m, 1H, Q-H), 7.23 (m, 1H, Q-H), 7.34 (m, 4H, Q-H, 3 × Ar-H), 8.01 (m, 4H, Q-H, 3 × Ar-H), 8.13 (m, 1H, Q-H), 8.20 (m, 1H, Q-H), 8.42 (m, 2H, 2 × An-H), 8.50 (m, 2H, 2 × An-H), 8.79 (s, 1H, An-H); ^{13}C-NMR (100 MHz, $CDCl_3$, 25 °C, TMS, δ): 139.37, 131.16, 131.01, 128.93, 127.58, 114.16, 71.89, 68.23, 42.92, 38.80, 33.56, 30.52, 29.79, 28.48, 27.80, 26.82, 25.97, 23.82, 22.80, 19.24, 14.22; ESI-MS (m/z): 891 (32 %) [**2**]$^+$. Anal. Calcd. for $C_{58}H_{62}N_6O_3$: C, 78.17; H, 7.01; N, 9.43 %. Found: C, 78.10; H, 7.07; N, 9.48 %.

Synthesis of 3: To a solution of **L_1** (0.36 g; 0.5 mmol) in dry acetonitrile (20 ml), anhydrous K_2CO_3 (1.5 g, excess) was added and stirred for 15 min. Freshly recrystallized 2-bromomethyl quinoline[S3] (0.11 g, 0.5 mmol) was added to it along with a crystal of KI and the reaction mixture was allowed to reflux for 72 h. After cooling to RT, K_2CO_3 was removed by filtration. The red filtrate was evaporated to dryness under reduced pressure, washed several times with water and then extracted with $CHCl_3$. The organic layer, after drying over anhydrous Na_2SO_4, evaporated to dryness to obtain a dark red solid. Compound **3** was isolated as white solid through column chromatography.

Yield: 55(%); mp: 162 °C; ^{1}H-NMR (400 MHz, $CDCl_3$, 25 °C, TMS, δ): 0.85 (m, 4H, 2 × CH_2), 1.40 (m, 8H, 4 × CH_2), 1.56 (m, 4H, 2 × CH_2), 2.34 (s, 2H, CH_2), 3.02-3.11 (m, 8H, 4 × CH_2), 4.24 (s, 4H, 2 × CH_2), 4.97 (br, 1H, NH), 5.95 (s, 2H, Q-CH_2), 6.64 (d, 1H, 1 × D-H), 6.79 (m, 5H, 2 × Q-H, 3 × Ar-H), 7.07 (m, 5H, 2 × Q-H, 3 × Ar-H), 7.16 (m, 2H, 2 × Q-H), 7.22 (m, 8H, 8 × Ar-H), 8.03 (d, 1H, 1 × D-H); ^{13}C-NMR (100 MHz, $CDCl_3$, 25 °C, TMS, δ): 166.01, 159.95, 157.33, 156.86, 143.49, 134.23, 132.87, 131.73, 130.52, 129.42, 128.66, 127.13, 125.81, 124.93, 123.62, 122.63, 120.97, 111.75, 110.70, 99.06, 66.59, 65.64, 56.89, 55.97, 54.79, 53.56, 52.44, 47.74, 46.60, 45.52, 29.78, 28.83; ESI-MS (m/z): 864 (38 %) [**3**]$^+$. Anal. Calcd. for $C_{49}H_{53}N_9O_6$: C, 68.12; H, 6.18; N, 14.59 %. Found: C, 68.18; H, 6.13; N, 14.61 %.

Physical measurements

Compounds **L, 1, 2 and 3** were characterized by elemental analyses, ^{1}H-NMR, ^{13}C-NMR and mass (positive ion) spectroscopy. ^{1}H-NMR and ^{13}C-NMR spectra were recorded on a JEOL JNM-LA400 FT (400 MHz and 100 MHz respectively) instrument in $CDCl_3$. ESI mass spectra were recorded on a WATERS Q-TOF Premier mass spectrometer. The ESI capillary was set at 2.8 kV and the cone voltage was 30V. Melting points were determined with an electrical melting point apparatus by PERFIT, India and were uncorrected. UV-visible spectra were recorded on a JASCO V-570 spectrophotometer at 293 K and the average of three measurements were taken. The deviations in molar absorption coefficients were in the last digit only. Steady-state fluorescence spectra were obtained using a Perkin-Elmer LS 50B Luminescence Spectrometer at 293 K with excitation and emission band-pass 5 nm. Steady-state fluorescence anisotropy data were obtained using a Perkin-Elmer LS 55 Fluorimeter at 293 K with slit width 5 nm and integration time 40 sec. Time-resolved fluorescence decays were recorded in a time-correlated single photon counting (TCSPC) system from IBH, with λ_{ex} = 295 nm. The fluorescence decays were collected with the emission polarizer at a magic angle of 54.7° and analyzed by using IBH DAS 6.2 software.

Fluorescence quantum yields of all the compounds were determined by comparing the corrected spectrum with that of anthracene (ϕ =0.297) in ethanol[S5] taking the area under the total emission. On the other hand, emission quantum yields due to diazole fluorophore in **L** and **3** were checked by comparing the corrected spectrum with that of quinine sulfate[S5] in 1N H_2SO_4. The complex stability constant K_s were determined[S6] from the change in absorbance or fluorescence intensity resulting from the titration of dilute solutions (~10^{-5}–10^{-6} M) of the fluorophoric systems against metal ion concentration. The reported values gave good correlation coefficients (≥0.98).

References

S1. K. G. Ragunathan, P. K. Bharadwaj, *Tetrahedron Lett.* 1992, **33**, 7581.

S2. (a) B. Bag, P. K. Bharadwaj, *Inorg. Chem.* 2004, **43**, 4626. (b) K. K. Sadhu, B. Bag, P. K. Bharadwaj, *Inorg. Chem.* 2007, **46**, 8051.

S3. K. N. Campbell, J. F. Ackrrman, B. K. Campbell, *J. Am. Chem. Soc.* 1949, **71**, 2905.

S4. M. Bullpit, W. Kitching, D. Doddrell, W. Adcock, *J. Org. Chem.* 1976, **41**, 760.

S5. Birks, J. B. *Photophysics of Aromatic Molecules*, Wiley-Interscience, New York, 1970.

S6. S. Fery-Forgues, M. -T. Le Bries, J. -P.Guetté, B. Valeur, *J. Phys. Chem.* 1988, **92**, 6233.

Captions for the Figures and Tables:

Fig. S1-S3:	ESI-MS, 400 MHz ^{1}H-NMR and 100 MHz ^{13}C-NMR spectra of **L**.
Fig. S4-S6:	ESI-MS, 400 MHz ^{1}H-NMR and 100 MHz ^{13}C-NMR spectra of **1**.
Fig. S7-S9:	ESI-MS, 400 MHz ^{1}H-NMR and 100 MHz ^{13}C-NMR spectra of **2**.
Fig. S10-S12:	ESI-MS, 400 MHz ^{1}H-NMR and 100 MHz ^{13}C-NMR spectra of **3**.
Fig. S13:	ESI-MS spectrum of **L**$\subset$Cu(II).
Table ST1-ST4:	Absorption and molar extinction coefficient (ε) of **L, 1, 2** and **3** in presence of different metal ions in MeCN.
Fig. S14-S16:	Absorption spectra of **1, 2** and **3** in presence of selected metal ions in MeCN.
Fig. S17-S19:	Emission spectra of **1, 2** and **3** in presence of selected metal ions in MeCN.
Table ST5:	Fluorescence output of **1, 2** and **3** with different ionic inputs
Fig. S20:	Plot of fluorescence quantum yield of **L** as a function of Cu(II) added in MeCN.
Fig. S21:	Emission spectra of anthracene of **L** in presence of Cu(II) ionic input in MeCN.
Fig. S22-S23:	Emission spectra of **1** in presence of Cu(II) ionic input and plot of fluorescence quantum yield of **1** as a function of Cu(II) added in MeCN.
Fig. S24:	Linear regression plots for complex stability constant determination of **1** in presence of Cu(II) inputs in MeCN.
Fig. S25:	Normalized overlap of absorption spectra of anthracene fluorophore with cryptand and emission spectra of quinoline fluorophore with cryptand in presence of different ionic inputs in MeCN.
Table ST6:	Fluorescence anisotropy data of the systems **L** and its metal complexes.
Table ST7:	Time resolved fluorescence decay analysis.

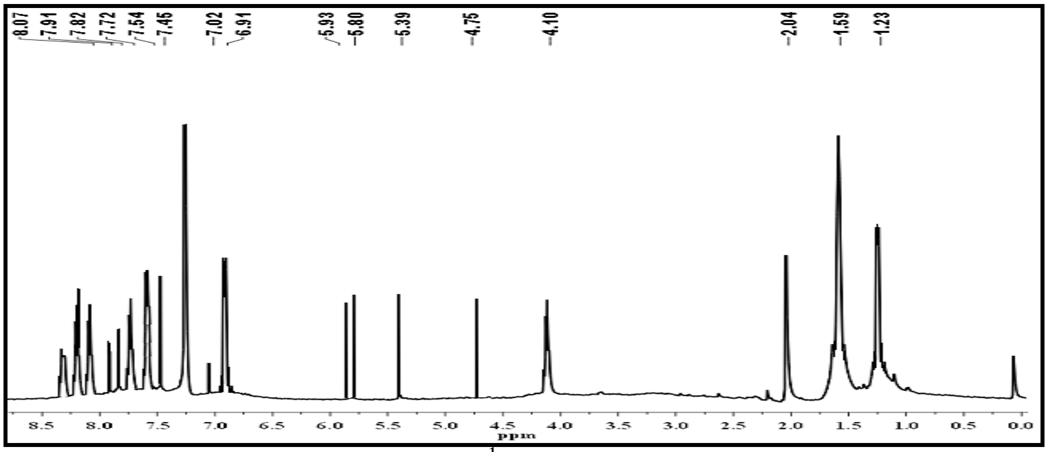

Fig. S1: 400 MHz ^{1}H-NMR spectrum of **L**.

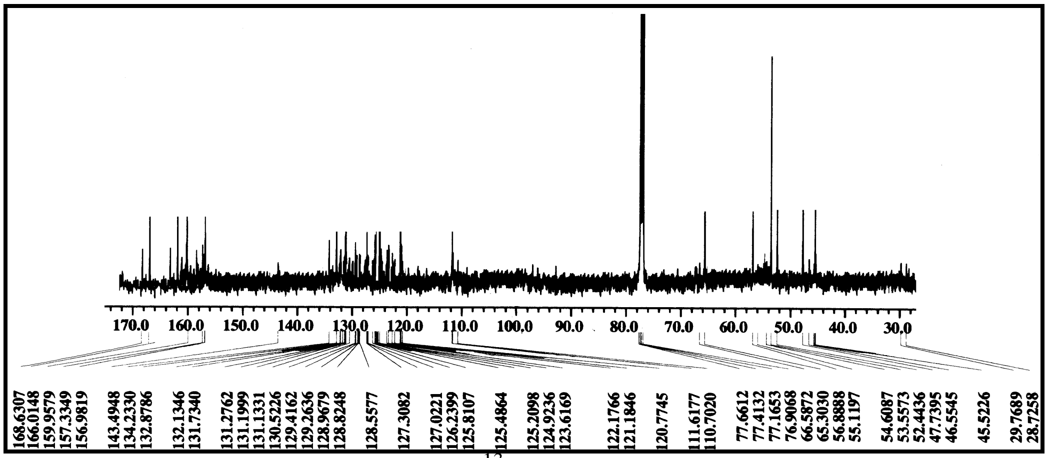

Fig. S2: 100 MHz ^{13}C-NMR spectrum of **L**.

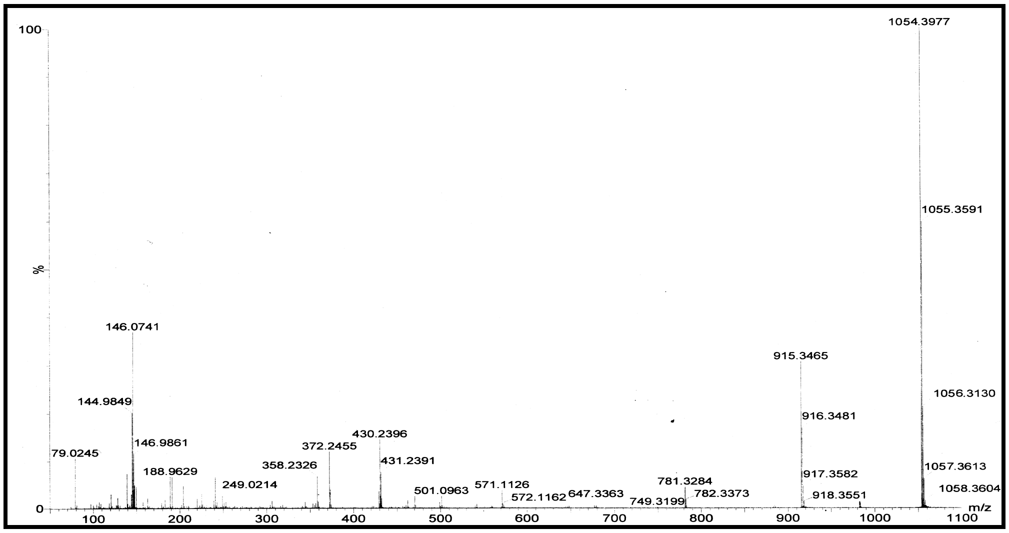

Fig. S3: ESI-MS spectrum of **L**.

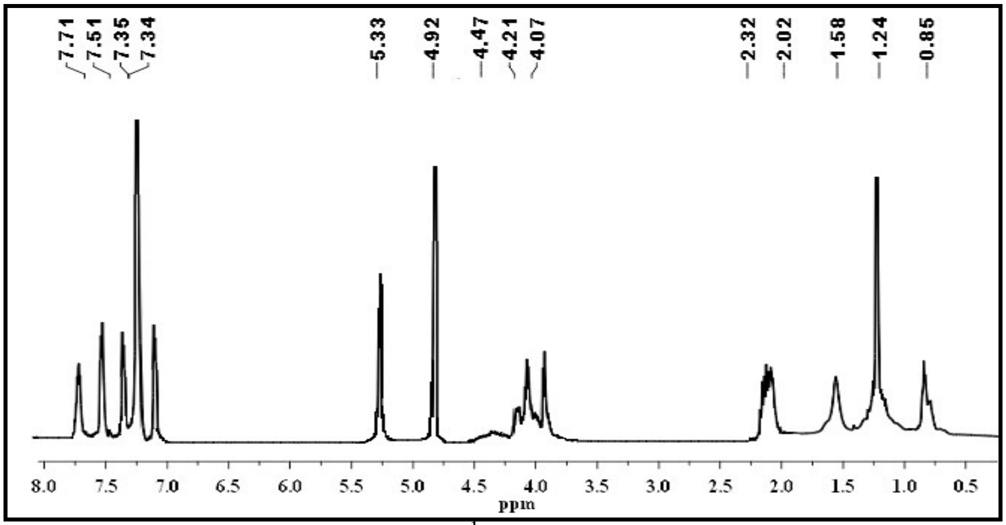

Fig. S4: 400 MHz ^{1}H-NMR spectrum of **1**.

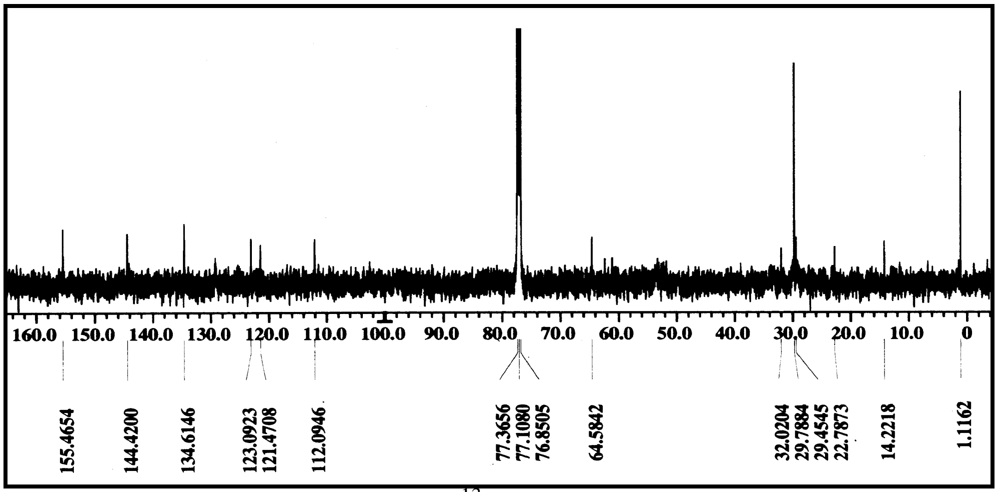

Fig. S5: 100 MHz ^{13}C-NMR spectrum of **1**.

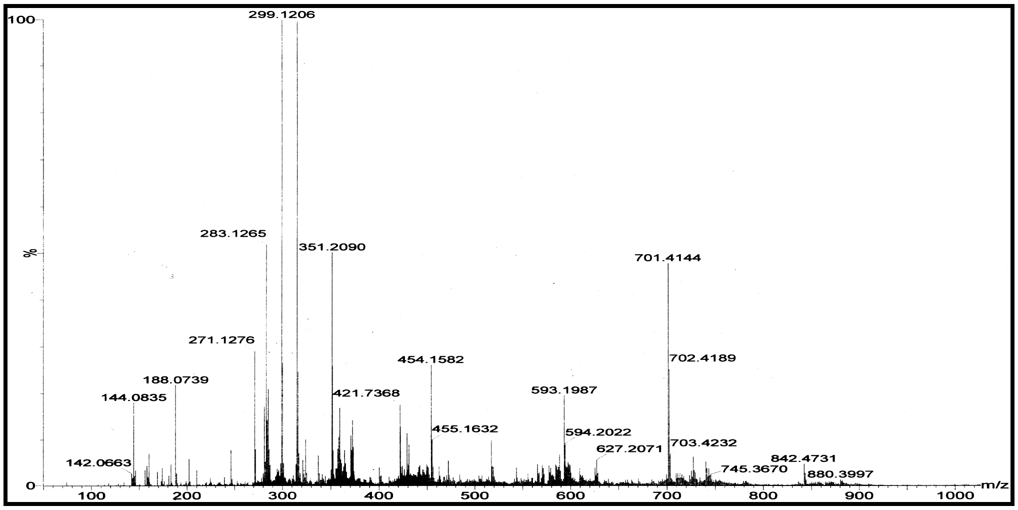

Fig. S6: ESI-MS spectrum of **1**.

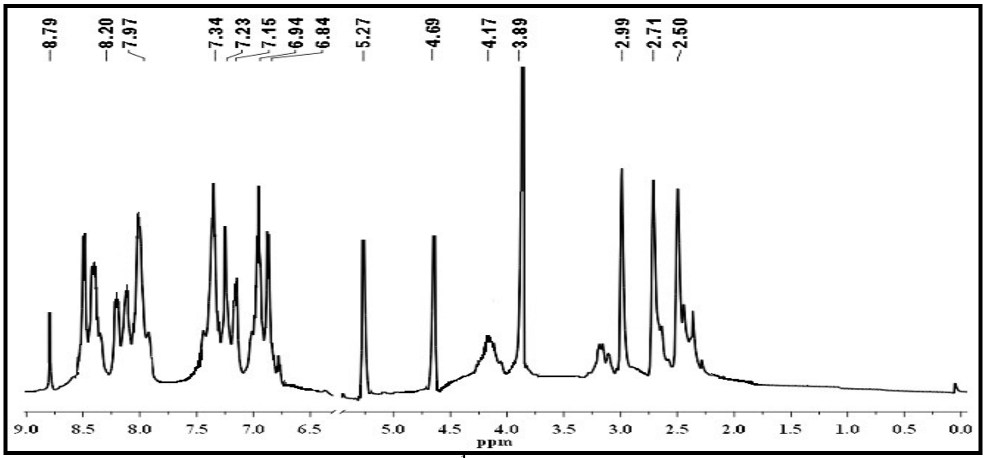

Fig. S7: 400 MHz ^{1}H-NMR spectrum of **2**.

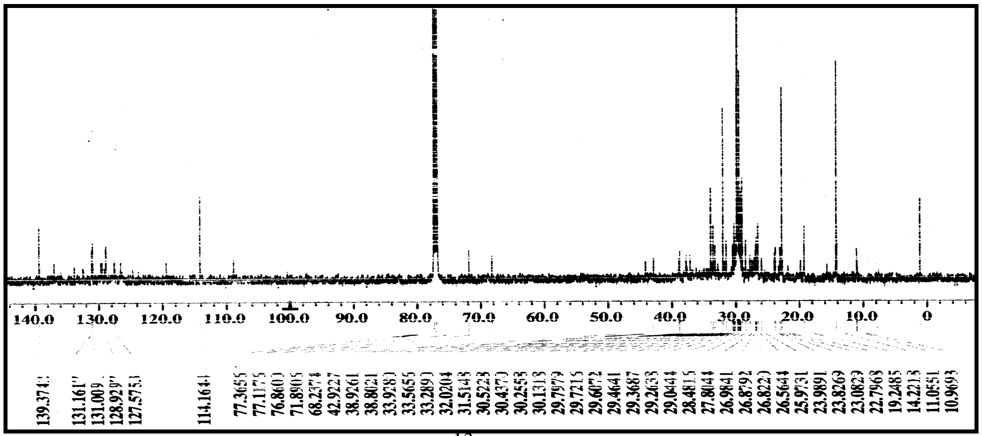

Fig. S8: 100 MHz ^{13}C-NMR spectrum of **2**.

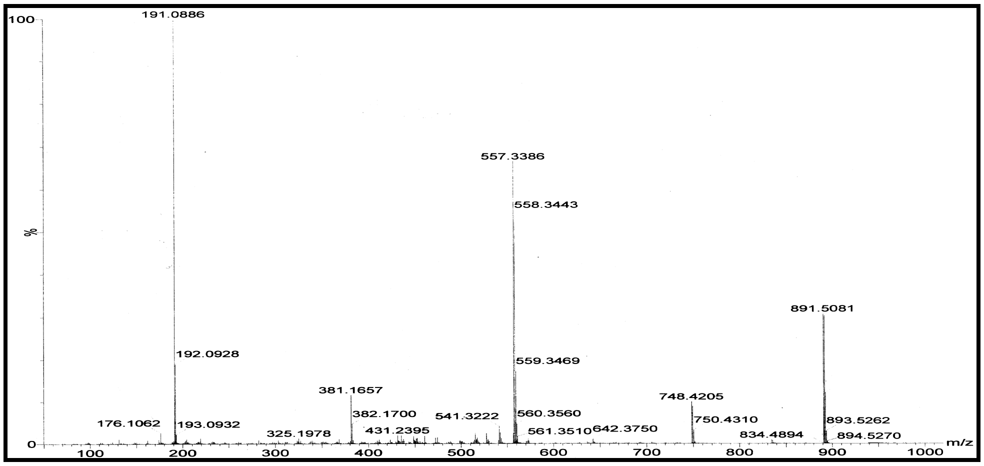

Fig. S9: ESI-MS spectrum of **2**.

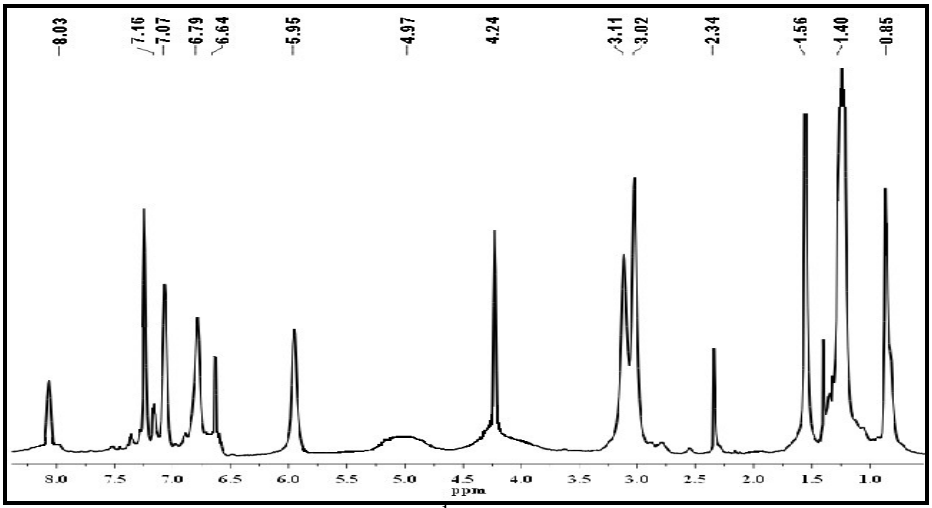

Fig. S10: 400 MHz ^{1}H-NMR spectrum of **3**.

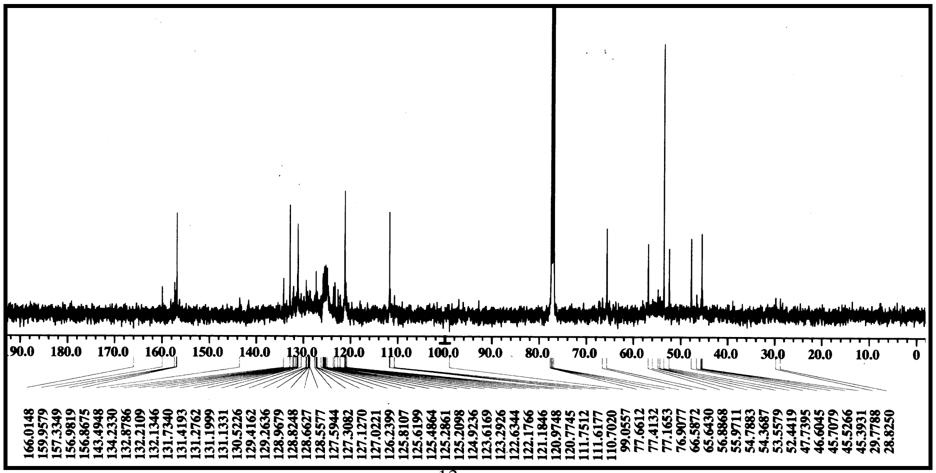

Fig. S11: 100 MHz ^{13}C-NMR spectrum of **3**.

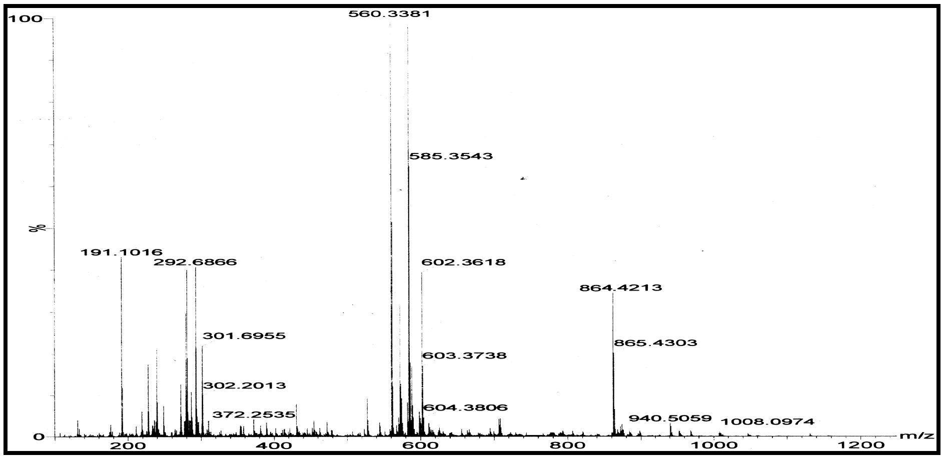

Fig. S12: ESI-MS spectrum of **3**.

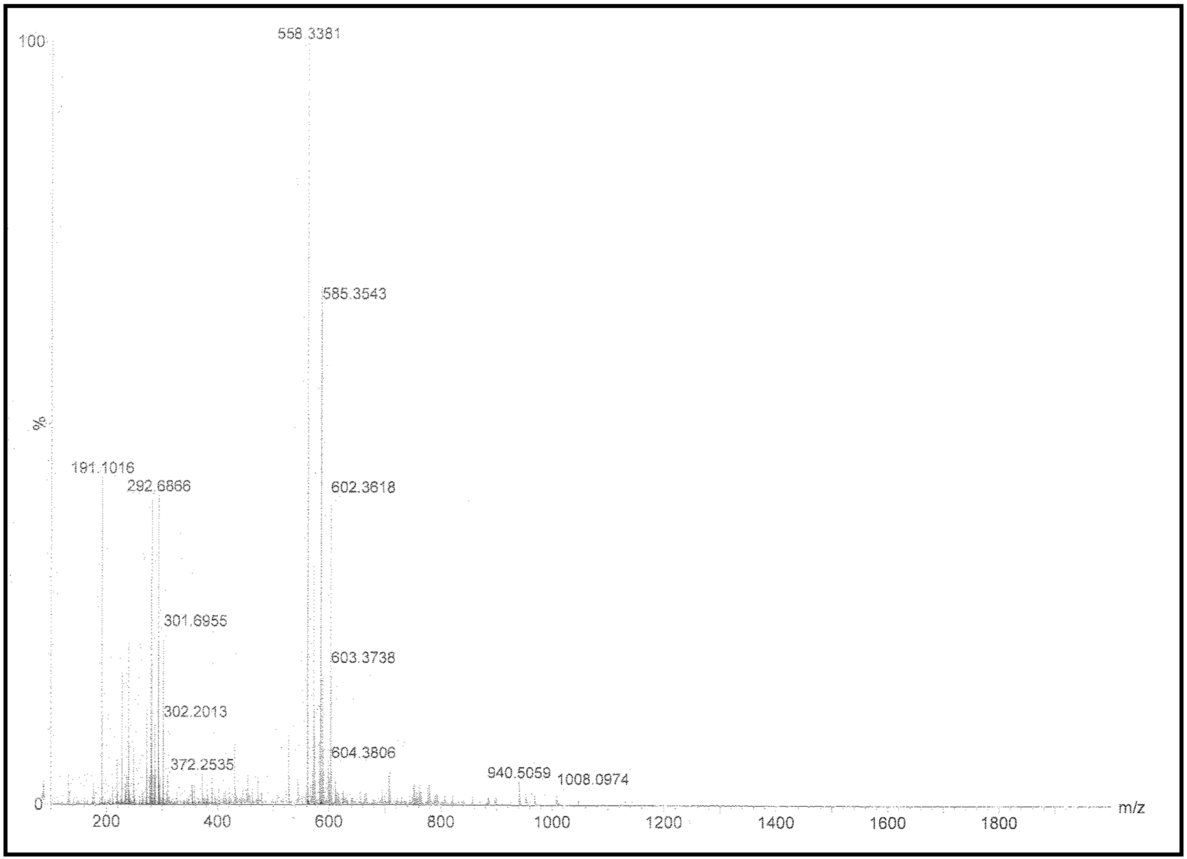

Fig. S13: ESI-MS spectrum of **L**$\subset$Cu(II) ESI-MS (m/z): 558 (100 %) [**L**$\subset$Cu]$^{+2}$.

Table ST1: Absorption and molar extinction coefficient (ε) of **L** with metal ions in MeCN (conc. of **L** = 1.2×10^{-5} M).

	Absorption λ, nm (ε, dm^3 mol^{-1} cm^{-1})					
L	476 (3703)	388 (3597)	346 (6412)	315 (9366)	272 (21011)	
L+Mn(II)	466 (3383)	390 (3199)	346 (5568)	314 (8550)	272 (18347)	
L+Fe(II)	477 (6646)	378 (29188)	336 (45949)	322 (52072)	285 (74568)	
L+Co(II)	471 (5833)	314 (10942)	264 (50288)			
L+Ni(II)	471 (4229)	375 (5052)	341 (7583)	315 (10083)	271 (23348)	
L+Cu(II)	460 (3198)	381 (6363)	315 (26813)	278 (31746)		
L+Zn(II)	465 (4602)	394 (4939)	375 (6187)	318 (12647)	272 (21881)	
L+Cd(II)	472 (4747)	383 (5126)	363 (6218)	343 (8238)	314 (12803)	274 (24999)
L+Ag(I)	455 (4466)	372 (5741)	355 (6584)	342 (7850)	316 (11126)	273 (20478)
L+Tl(I)	470 (3750)	376 (4174)	343 (6355)	314 (8502)	272 (19253)	
L+H$^+$	452 (4832)	373 (7071)	320 (13752)	273 (20425)		

Table ST2: Absorption and molar extinction coefficient (ε) of **1** with metal ions in MeCN (conc. of **1** = 1.8×10^{-4} M).

	λ, nm (ε, $dm^3\ mol^{-1}\ cm^{-1}$)		
1	314 (12021)	301 (10926)	266 (14187)
1+Mn(II)	314 (12639)	301 (11548)	267 (13839)
1+Fe(II)	320 (18068)	297 (20326)	
1+Co(II)	314 (12521)	301 (11422)	267 (14079)
1+Ni(II)	314 (12993)	301 (11947)	268 (14120)
1+Cu(II)	297 (18565)	253 (22467)	
1+Zn(II)	303 (17365)		
1+Cd(II)	315 (11518)	302 (10474)	269 (10029)
1+Ag(I)	314 (14015)	301 (13218)	269 (12808)
1+Tl(I)	314 (12327)	301 (11340)	266 (14735)
1+H^+	302 (16770)		

Table ST3: Absorption and molar extinction coefficient (ε) of **2** with metal ions in MeCN (conc. of **2** = 0.8×10^{-5} M).

	Absorption λ, nm (ε, $dm^3\ mol^{-1}\ cm^{-1}$)						
2	384 (1420)	364 (1709)	333 (2088)	313 (4353)	300 (6231)	272 (13873)	
2+Mn(II)	380 (2216)	364 (2482)	343 (3731)	310 (8524)	274 (13196)		
2+Fe(II)	384 (2289)	359 (2968)	346 (3521)	315 (8428)	301 (9850)	273 (15104)	
2+Co(II)	481 (2715)	384 (1658)	364 (1826)	344 (2265)	314 (5118)	300 (7320)	273 (14581)
2+Ni(II)	392 (1378)	372 (2021)	345 (2148)	313 (4653)	301 (6195)	272 (13883)	
2+Cu(II)	317 (31670)	253 (421750)					
2+Zn(II)	377 (2669)	343 (2875)	316 (8199)	302 (9950)	272 (14533)		
2+Cd(II)	381 (2105)	363 (2111)	343 (2619)	313 (6350)	300 (8524)	271 (14248)	
2+Ag(I)	385 (1961)	364 (2400)	343 (3353)	317 (7405)	303 (8813)	271 (13314)	
2+Tl(I)	382 (2599)	364 (3215)	344 (3480)	313 (5959)	301 (7905)	271 (16824)	
2+H^+	373 (2419)	343 (3731)	314 (8498)	274 (13196)			

Table ST4: Absorption and molar extinction coefficient (ε) of **3** with metal ions in MeCN (conc. of **3** = 7.6×10^{-5} M).

	λ, nm (ε, $dm^3\ mol^{-1}\ cm^{-1}$)				
3	474 (3533)	337 (2756)	317 (4206)	293 (4415)	275 (5199)
3+Mn(II)	470 (3334)	334 (5020)	316 (4355)	296 (4418)	275 (5133)
3+Fe(II)	469 (2955)	333 (4804)	317 (4279)	296 (4298)	273 (5038)
3+Co(II)	472 (3875)	335 (5173)	318 (4662)	296 (4788)	274 (5567)
3+Ni(II)	472 (3334)	336 (4925)	318 (4327)	296 (4363)	274 (5211)
3+Cu(II)	466 (1781)	337 (5926)	317 (7480)	282 (13661)	
3+Zn(II)	466 (2360)	330 (5366)	317 (5026)	297 (4642)	274 (5112)
3+Cd(II)	472 (3141)	335 (4766)	319 (4414)	297 (4504)	276 (4959)
3+Ag(I)	467 (2484)	327 (6172)	309 (4738)	296 (4042)	275 (4484)
3+Tl(I)	473 (3519)	336 (5207)	317 (4611)	297 (4783)	275 (5778)
3+H$^+$	459 (2389)	322 (6538)	297 (4129)	274 (4270)	

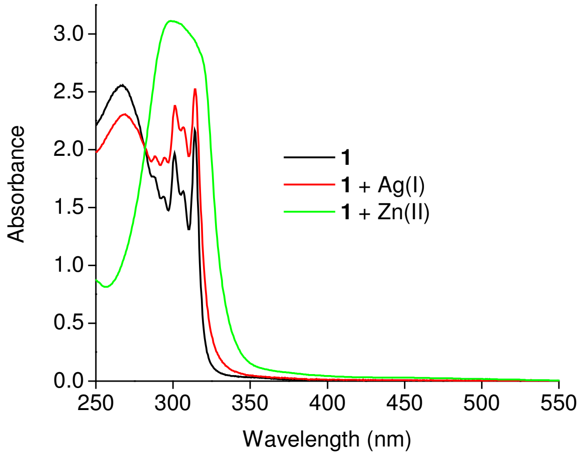

Fig. S14: UV-vis spectrum of **1**, **1**+Zn(II), **1**+Ag(I) (conc. of **1** = 1.8×10^{-4} M) in MeCN.

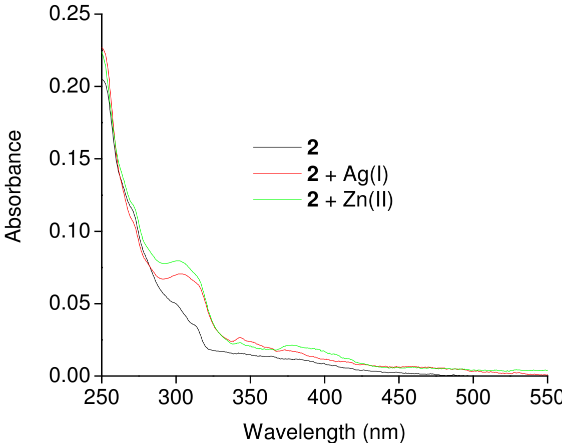

Fig. S15: UV-vis spectrum of **2**, **2**+Zn(II), **2**+Ag(I) (conc. of **2** = 0.8 × 10^{-5} M) in MeCN.

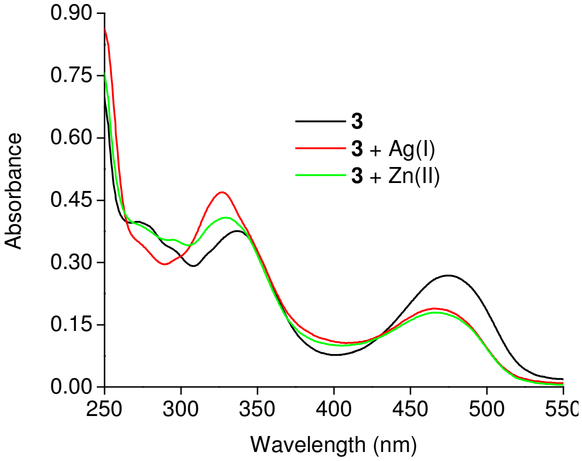

Fig. S16: UV-vis spectrum of **3**, **3**+Zn(II), **3**+Ag(I) (conc. of **3** = 7.6 × 10^{-5} M) in MeCN.

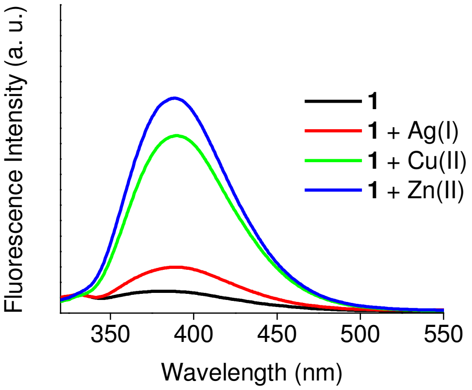

Fig. S17: Emission spectrum of **1**, **1**+Cu(II), **1**+Zn(II), **1**+Ag(I) (conc. of **1** = 1.0 × 10^{-6} M) in MeCN.

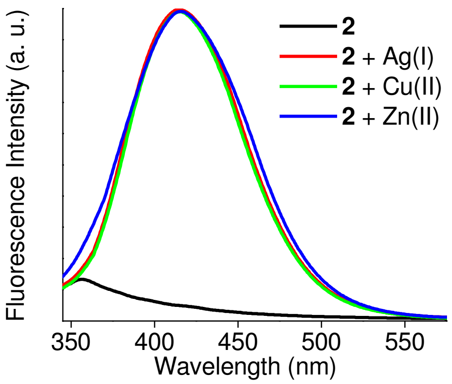

Fig. S18: Emission spectrum of **2**, **2**+Cu(II), **2**+Zn(II), **2**+Ag(I) (conc. of **2** = 1.0 × 10^{-6} M) in MeCN.

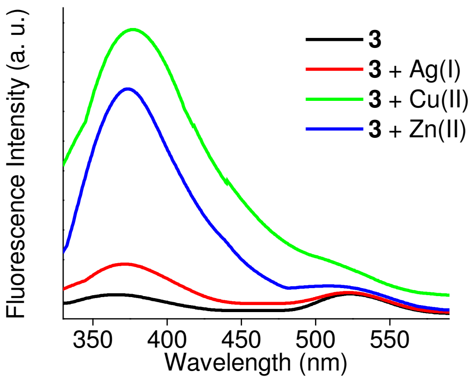

Fig. S19: Emission spectrum of **3**, **3**+Cu(II), **3**+Zn(II), **3**+Ag(I) (conc. of **3** = 1.0 × 10^{-6} M) in MeCN.

Table ST5: Fluorescence output of **1, 2** and **3** with different ionic inputs

Inputs	Quantum Yield φ (Enhancement Factor) (λ_{ex}= 316 nm)				
	1	**2**		**3**	
	ϕ_{Quin}	ϕ_{Quin}	ϕ_{Anthr}	ϕ_{Quin}	ϕ_{Diaz}
None	0.0020	0.0008	0.0014	0.0020	0.0020
Mn(II)	0.0536 (27)	0.0016 (2)	0.0981 (70)	0.0280 (14)	0.0056 (3)
Fe(II)	0.0860 (43)	0.0026 (3)	0.1727 (123)	0.0290 (15)	0.0054 (3)
Co(II)	0.0896 (45)	0.0011 (1)	0.0573 (41)	0.0290 (15)	0.0047 (2)
Ni(II)	0.0692 (35)	0.0007 (<1)	0.0242 (17)	0.0266 (13)	0.0033 (2)
Cu(II)	0.1086 (54)	0.0033 (4)	0.2145 (153)	0.1768 (88)	0.0301 (15)
Zn(II)	0.1296 (65)	0.0037 (5)	0.2287 (163)	0.1216 (61)	0.0322 (10)
Cd(II)	0.0126 (6)	0.0019 (2)	0.1174 (84)	0.0166 (8)	0.0031 (2)
Ag(I)	0.0068 (3)	0.0034 (4)	0.2205 (158)	0.0322 (16)	0.0023 (1)
Tl(I)	0.0704 (35)	0.0008 (1)	0.1554 (111)	0.0186 (9)	0.0016 (<1)
H^+	0.0068 (3)	0.0038 (5)	0.1320 (94)	0.0069 (3)	0.0440 (14)

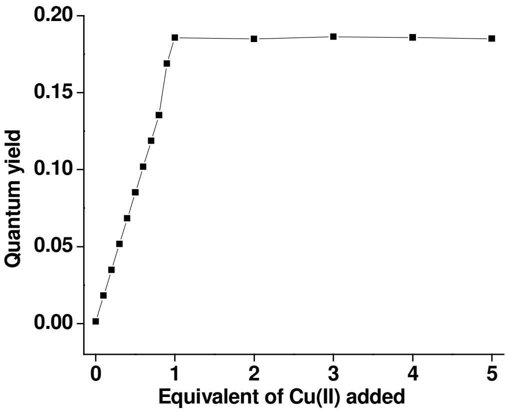

Fig. S20: Plot of fluorescence quantum yield of diazole of **L** as a function of Cu(II) added in MeCN.

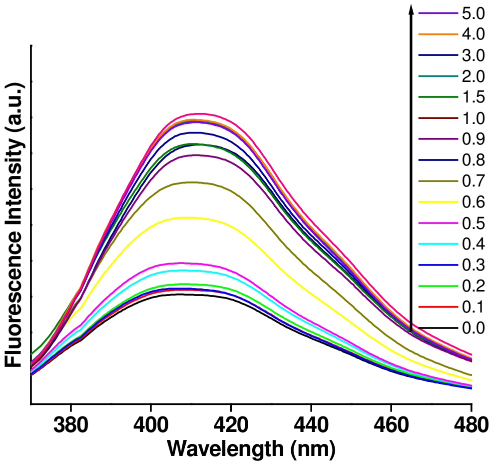

Fig. S21: Emission spectra of anthracene of **L** in presence of Cu(II) ionic input in MeCN.

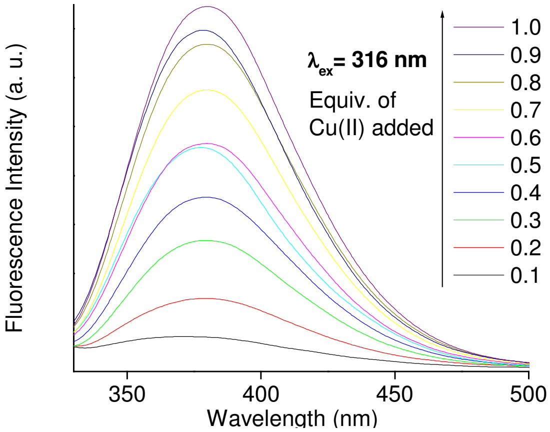

Fig. S22: Emission spectra of **1** in presence of Cu(II) ionic input in MeCN.

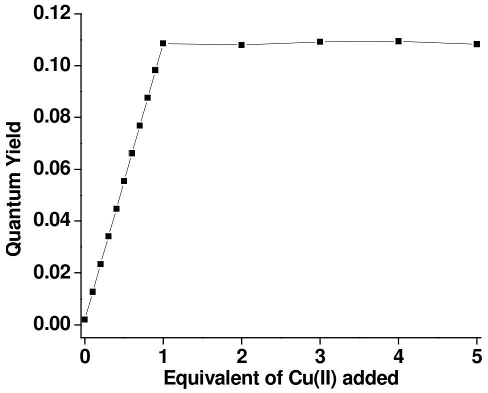

Fig. S23: Plot of fluorescence quantum yield of **1** as a function of Cu(II) added in MeCN.

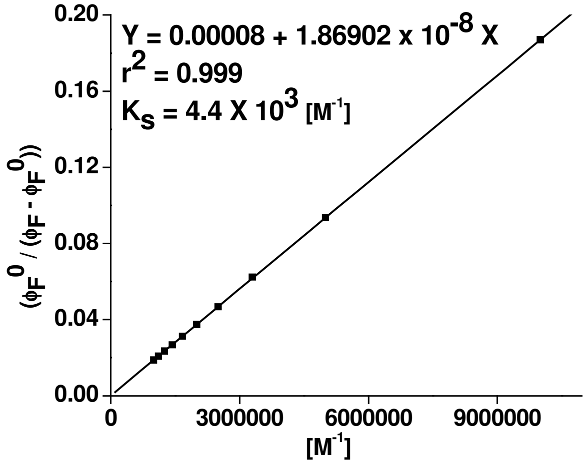

Fig. S24: Linear regression plots for complex stability constant determination of **1** in presence of Cu(II) input in MeCN.

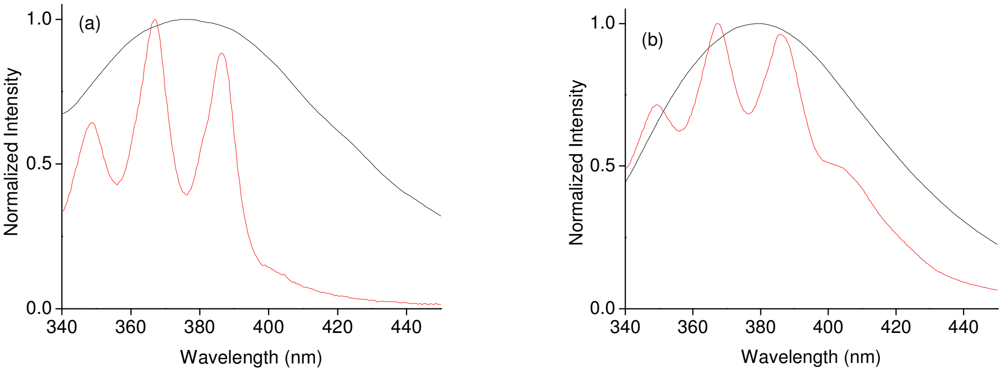

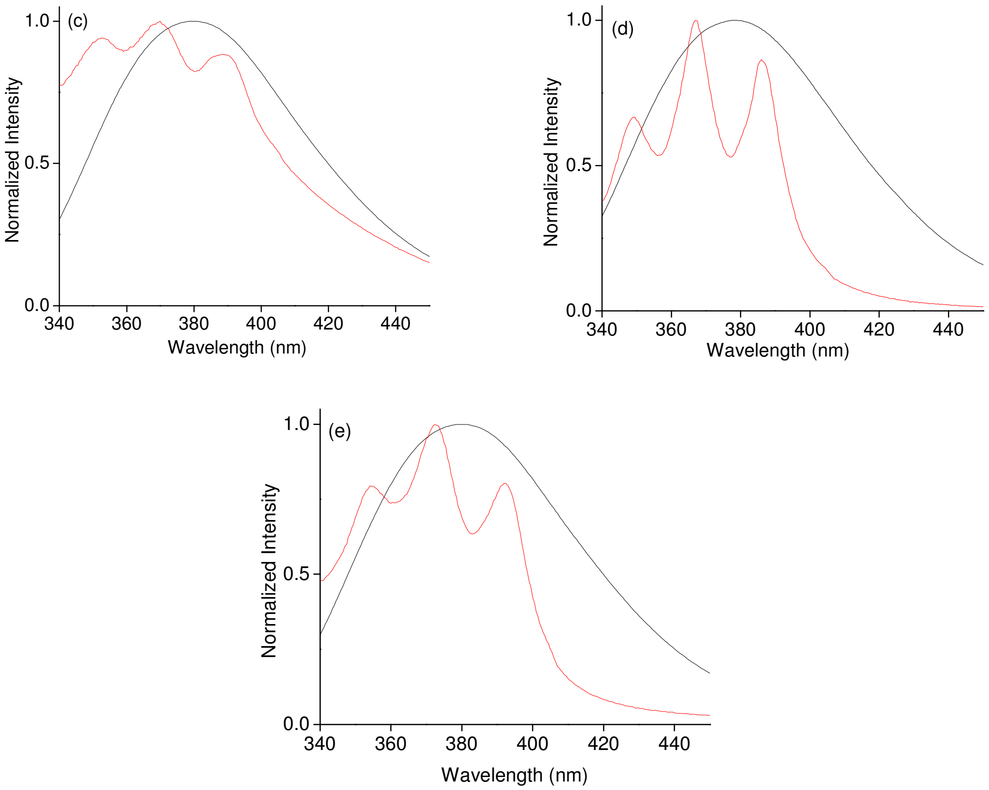

Fig. S25: Normalized overlap of absorption spectra of anthracene fluorophore with cryptand (red line) and emission spectra of quinoline fluorophore with cryptand (black line) (a) alone and in presence of (b) Ag(I), (c) Cu(II), (d) Zn(II) and H^+ in MeCN.

Table ST6: Fluorescence anisotropy data of the systems **L** and its metal complexes.

(a) Excitation at 316 nm

Sample	Anisotropy(Donor)	Anisotropy(Acceptor)
L	0.39	0.45
L + Zn(II)	0.30	0.40
L + Cu(II)	0.30	0.40
L + Ag(I)	0.31	0.41
L + H^+	0.35	0.43

(b) Excitation at 340 nm

Sample	Anisotropy(Donor)	Anisotropy(Acceptor)
L	0.26	0.03
L + Zn(II)	0.22	0.12
L + Cu(II)	0.22	0.05
L + Ag(I)	0.20	0.10
L + H^+	0.25	0.35

Table ST7: Time resolved fluorescence decay analysis

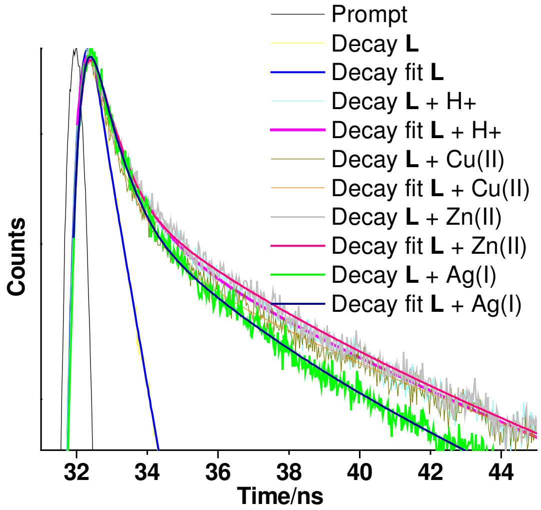

λ_{ex} = 295 nm; λ_{em} = 418 nm

Sample	A_1	T_1	A_2	T_2	A_3	T_3	X^2
L	0.53	0.20	0.10	1.36	0.37	3.89	1.01
L + Ag(I)	0.58	0.56	0.13	4.47	0.29	27.19	1.07
L + Cu(II)	0.49	0.95	0.09	6.77	0.43	31.29	1.11
L + Zn(II)	0.55	0.59	0.12	5.30	0.33	30.93	1.08
L + H^+	0.46	0.97	0.13	6.36	0.41	31.04	1.06

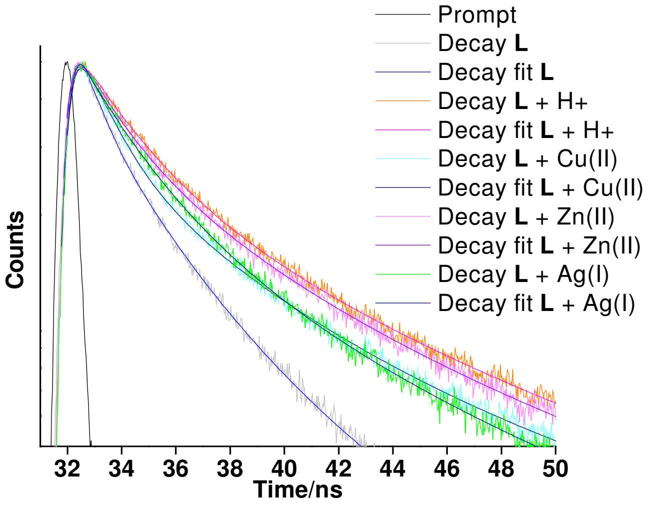

λ_{ex} = 295 nm; λ_{em} =518 nm

Sample	A_1	T_1	A_2	T_2	A_3	T_3	X^2
L	0.42	0.57	0.42	2.81	0.15	9.62	1.07
L + Ag(I)	0.54	2.25	0.34	6.77	0.11	24.8	1.09
L + Cu(II)	0.55	1.2	0.34	5.71	0.11	27.08	1.08
L + Zn(II)	0.50	2.27	0.36	7.7	0.14	27.95	1.05
L + H^+	0.45	1.79	0.40	6.38	0.15	24.52	1.05